A Unified Fatigue and Fracture Model applied to Steel Wire Ropes

Prof. M.P. Weiss and Dr.R. Ashkenazy
Faculty of Mechanical Engineering, Technion IIT
Haifa 32000, Israel e-mail: mweiss@technion.ac.il

ABSTRACT

The behavior of short and very short fatigue cracks, emanating from "smooth" specimens has been an intriguing research topic for a long time. A prediction of propagation of such cracks and its industrial application has been scarce. A quantitative two-term model for a step by step simulation of crack propagation from very short cracks to final fracture has been proposed by one of the authors. The model is based on the Fatigue Diagram that segregates the whole fatigue and fracture domain into 6 unique zones, and relates each zone to a known fatigue and/or fracture regime. Zone 4 in the diagram is so bounded that the stress amplitudes are higher than the endurance stress, but lower than the elastic limit, and the stress intensity factor ranges are higher than the threshold and lower than the fracture toughness. Most metal parts and structures finally break down in this zone by critical crack propagation, or climb up into the plastic zone 6 and fail there by gross yielding. In zone 4 the superposition of two fatigue crack propagation rules is postulated and used. The fatigue model is described, discussed and enhanced. It is shown to be applicable to fatigue failure in single wires of steel wire ropes in general and specifically in non-rotating tower crane wire ropes. The individual wires in a steel wire rope are subjected to fluctuating tension loading and to bending over sheaves. These bending stresses along the individual double helix wire are strongly dependent on the sheave-to-wire diameters ratio and on the arrangement of the reeving system. It is assumed that initial flaws that were generated during the cold drawing manufacturing process exist in the individual wire. An un-lubricated rope is assumed. Accordingly, relative displacements between adjacent wires are not permitted. The theoretical results were tested on industrial wires, using a specially built tension apparatus that was free to rotate on one end, so that the twisting moments and deformations that were generated by tension, could be measured. The results of the measured stresses were found to be close to the analytical predictions. The simulated fatigue life was found to be in good agreement with experimental results.

Introduction

Fatigue and fracture of materials and structures are very complex phenomena and a function of many parameters. Research activities in these fields have been performed for more than 150 years, since the pioneering study of Wohler on railway axles. A general analytic solution to fatigue problems has not been found yet, and the advancement of materials science and technology has made the domain even more complex and challenging than before. The research extends over specific areas such as: fracture mechanics, multi mode, damage mechanics, high cycle, low cycle, overloads, materials response and many others. Hundreds of researchers have performed thorough studies, published thousands of papers and numerous books, and therefore many specific problems have been practically solved, airplanes are safely flying and structures are maintaining their rigidity, but the basic phenomenon is still not adequately understood and more often than not cannot be predicted with sufficient accuracy. It is the aim of this study to try and tackle the general fatigue and fracture domain and problem, sort it into separate zones and regimes, and present possible, some well known, directions how to deal with the problem in each regime. Most well known fatigue phenomena will be quantitatively explained by the zone separation. One practical, previously unsolved problem, namely the fatigue of a regular, double-helix steel wire, will be analyzed and simulated and shown to be a good example of a structure that lies in zone 4 of the fatigue domain.

The fatigue and fracture domain

The three zones of elastic (LEFM) plastic (EPFM) and micro-structural (MPM) fracture mechanics in relation to stress levels, were qualitatively introduced and portrayed by Miller [1;2]. He described a qualitative picture that was used to explain the relations between the different fatigue regimes, including short and very short cracks that started to get attention at that time. It was not possible to use this map for quantitative description nor for clarification of the various phenomena, like for example the H-L and L-H sequence effect, the mean stress effect etc. For quantitative diagram a more detailed map is needed.

The numerous studies that were performed in the past have shown that the outer limits of the fatigue phenomenon, in the stress field are bounded by the ultimate tensile strength – S_U on one side and by zero stress amplitude on the lower side. In certain materials and structures no fatigue damage was observed below the "endurance limit" – S_E , but in other cases it was. So that the endurance limit cannot be considered as an outer limit of the fatigue domain, but it has to be included as an important part of it. In certain materials, like in aluminum, the endurance limit has not been observed at all, and some would argue that generally a fatigue limit does not exist. They claim that, if the tests would have been continued long enough with very high number of stress cycles, the specimen would eventually fail in fatigue. So the lower limiting stress should be zero.

The yield strength – S_Y is also an important parameter, in spite of the controversy whether such an idiom is justified to exist at all, and whether it is can be expressed as a fixed value or only as a bordered area in the stress field. Its importance lays in the fact that it is very broadly used in practical engineering as a starting point for safety factors. Therefore the yield strength has to be part of the general fatigue domain.

In fracture mechanics, the clear limit on the upper side is the fracture toughness – K_{1C}, at which all cracks propagate catastrophically and the structural cracked part is finally separated into two parts – therefore fails. On the lower side the limit is not very clear. Not long ago the stress intensity factor range threshold – ΔK_{TH} was considered as the lower limit, below which cracks do not propagate under cyclic loads. It is well known now that micro-cracks do propagate below the threshold too, and the so called "smooth" specimens develop fatigue cracks under cycling, high stresses and finally break. Therefore the lower limit of the fracture domain has to be decided as very low ΔK which is a function of stress amplitude and the crack length. Because the stresses vary, one has to set the crack length at its lowest practical value. For engineering purposes and our study this value in smooth parts can be set as ~1 micron, because very finely finished metal surfaces have indentations that are slightly higher than that, as shown by Taylor at al. [2]. Recently MEMS and NANO devices are considered against fatigue and fracture too, and therefore in future the relevant lower limit of the practical crack length will decrease.

All the above parameters define the whole domain of fatigue and fracture problematic, and to demonstrate this domain clearly one has to exhibit them on one simple diagram. As the fracture mechanics parameters of stress intensity factors are a function of specimen geometry, not material attributes, the diagram has to refer to one specific specimen and loading geometry, for example a mode I case. Any other specimen size geometry will have a slightly different diagram, and for mode II or mode III specimens the diagram can change more considerably. A general fatigue diagram for a tension-compression mode I specimen, with a surface micro-crack a, has been introduced by Weiss [3], and enhanced by Weiss and Hirshberg [4]. The diagram is depicted in Figure 1. This fatigue diagram includes the whole fatigue and fracture domain.

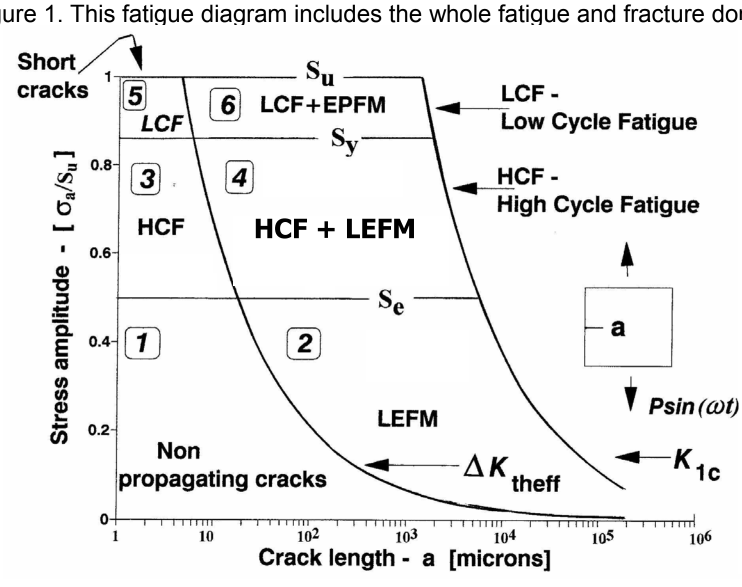

Figure 1. The fatigue diagram for a smooth specimen with a surface micro-crack a, under mode I tension-compression. The whole fatigue & fracture domain is divided depicted and divided into six zones and regimes

The Fatigue Zones and Regimes

As shown in Figure 1, the whole fatigue domain is depicted on one comprehensive diagram, for each one certain specimen geometry and loading function and material. It is shown with log a – the crack length, as the abscissa, and the normalized stress amplitude – σ_A/S_U as the ordinate. The log scale is used for the crack length, because micro-cracks of several microns have to be discriminated and final cracks of many millimeters or tens of centimeters have also to be clearly seen too. The stress amplitude is shown on linear scale. The ordinate is divided into three parts by constant stress lines of 0, S_U, S_Y and S_E

$$\Delta K = \Delta\sigma . Y(a)\sqrt{a\pi} \quad (1)$$

where

ΔK = the stress intensity factor range

$\Delta\sigma$ = the stress double amplitude

a = the crack length

$Y(a)$ = a dimensionless function of the crack length a

which emphasize the fact that the diagram is valid for a certain specimen and a certain material. Here it is assumed that S_y and S_E exist, as in low alloy steels and in many other metals. The fracture mechanics parameters are depicted as constant ΔK lines, calculated for the round (or rectangular) tension-compression specimen with mode I loading, based on the classical relation [1]. The constant ΔK lines that are shown on the diagram are the ΔK_{TH} line, and the line when the maximum stress intensity factor – K_{MAX} in the loading cycle equals K_{1C}, or also equals to maximum ΔK when the compression stresses have been neglected, as non-contributing to crack propagation. One could depict many other intermediate ΔK lines between the above mentioned two, but as it is shown it makes the picture clear. Now the whole domain has been divided into six distinct zones each of which comprises one unique fatigue regime, or a combination of such. The behavior of the specimen under cycling loads, namely the crack propagation, will be different in each zone, and will have to be calculated by a different procedure. The attributes of the different zones are as follows:

1. Zone 1 is below the endurance limit – S_E and to the left of the stress intensity factor range – ΔK_{TH} therefore no cracks propagate there, so it is the safe zone, or one with Non-Propagating cracks. It is also bordered by the well known Kitagawa [5] line.

2. Zone 2 is below the endurance limit – S_E, above the stress intensity factor threshold line - ΔK_{th}, and below the fracture toughness – K_{1C} line, therefore it is the classical LEFM – linear elastic fracture mechanics zone. Here the exponential Paris\` law fatigue crack propagation predictions, supply good fit to experimental results, with reasonable scatter only.

3. Zone 3 is above the endurance limit –S_e, below the yield stress line - S_y and to the left of the stress intensity factor threshold line – ΔK_{TH}, it is the elastic High Cycle fatigue zone. In classical fatigue tests on smooth specimens, all of which start in this zone, most of the cyclic lifetime is spent here. The lower the stress amplitude, the higher is the percentage of number of cycles that is spent in this zone, starting with more than 90 % close to the endurance limit, and much less than 50 % when the stress amplitude climbs up close to the yield stress. The length of the cracks in the specimens in this zone start from very low values, a few microns, and when leaving zone 3 the cracks are between 10 and 20 microns, depending on the material and the stress amplitude.

4. Zone 4 includes a combination of regimes. It is bounded by four lines: the endurance limit –S_E line from below, the yield stress line – S_Y from above, the stress intensity factor threshold line – ΔK_{TH} from the left and the fracture toughness – K_{1C} line from the right. As zone 4 is above the S_E, the High Cycle regime exists here. As zone 4 is above the ΔK_{TH} , the LEFM zone exist here also. So it is a combination of High Cycle fatigue and LEFM regimes. Practically all specimens pass zone 4 on their way from zones 2 or 3 to failure by critical crack propagation on line K_{1c}, or by gross yielding to zone 6. Using Paris\` law in zone 4 results with high scatter between calculation and experimental results, and the same happens if one uses High Cycle predictions. Only a type of superposition of the two calculation methods can systematically result with good predictions. This issue will be enlarged later on.

5. Zone 5 is in the plastic region, above the yield stress – S_Y and below the ultimate tensile strength S_U. It is also to the left of the stress intensity factor range threshold - ΔK_{TH} . So it is in the Low Cycle fatigue region. Only a combination of very smooth specimen and very high cycling stress will take place here. It is not a practical zone for engineering applications. A way how to predict crack propagation here has to be developed.

6. Zone 6 is again a combination of regimes. It is above the yield stress line – S_Y and below the ultimate tensile strength line – S_U. It also is between the stress intensity factor threshold line – ΔK_{TH} from the left and the fracture toughness – K_{1C} line from the right. So it is in the Low Cycle fatigue (LCF) regime and the fracture mechanics regime. It can be named as a combination of LCF and EPFM –(Elasto-Plastic Fracture Mechanics). Here also a practical way of crack propagation prediction has to be developed.

A convenient and clear advantage of the diagram and the model is that it enables to quantitatively predict and explain the fatigue crack propagation from the onset of loading till final separation, in a smooth metal specimen under tension-compression - the basic problem in fatigue, that was impossible to calculate before. Another advantage is that the model enables to build S-N curves for different materials, specimens and loading conditions, as will be shown later, after the details of the calculating equations will be shown and explained.

Crack propagation prediction

The crack propagation rate prediction da/dn in zone 2, the LEFM zone, has been calculated and predicted by eq. [2] :

$$(da/dn)_2 = C_2.\Delta K_{EFF}^2 (\frac{\Delta K_{EFF} - \Delta K_{TH}}{K_{1C} - \Delta K_{EFF}})^{\beta} \tag{2}$$

where

C_2 = a material parameter
ΔK_{EFF} = is the effective stress intensity factor range
B = is an exponent that governs the curvature of da/dn line near K_{1C} and ΔK_{TH}
ΔK_{TH} = is the threshold stress intensity factor range
K_{1C} = is the fracture toughness

This is a modified Paris` law, that predicts not only the incline of the da/dn line, but also the curvature near its both ends, the one near $K_{1C}$, and the other near $\Delta K_{TH}$. It is comparable to some other modifications to the Paris` law, many of which have been proposed in the literature. One could use different exponents for the numerator in eq. [2] which govern the curvature near the threshold, and the denominator which governs the curvature near K_{1C}, but it was found that in low alloy steels, using the number β = 8 for both sides, resulted with good fit. It can be changed for other cases. The regular exponent of ΔK that is used in experimental fit of the Paris` law is around 3, but here the initial exponent of ΔK is set as 2, so that an analytical derivation of this relation will be possible in the future. In eq. [2] the expression in the parentheses, brings this exponent to be close to 3 in the mid range of ΔK, and compensates it near the boundaries.

The crack propagation prediction rate da/dn in zone 3, the High Cycle zone, has been calculated and predicted by eq. [3]:

$$(da/dn)_3 = C_3.a.\sigma_a^2 (\frac{\sigma_a - S_E}{S_U - \sigma_a})^{\gamma} \tag{3}$$

where

C_3 = a material parameter
a = is the crack length
σ_a = is the stress amplitude
S_E = is the endurance limit
S_U = is the ultimate tensile strength
γ = is an exponent that governs the curvature of the da/dn line near S_E and S_U

This relation is not an established general solution, but it was successfully used in zone 3 and resulted with good predictions, in steels, aluminum and magnesium. The exponent γ was set here also as 8 as in zone 2. The influence of the curvature in the high end i.e. near S_U and K_{1C}, is very small, but in the low ends its influence is substantial.

It is important to mention that the stress amplitude that is used for calculations is different for the two parts. In eq. [2] which is based on fracture mechanics principles, it is based on the remote stress amplitude, which is not affected by the crack propagation, and therefore stays constant during the simulation process. The SIF increases only as a function of the crack length a. The stress amplitude - σ_a used in eq. [3], is based on the engineering stress at the vicinity of the tip of the crack (at the end of the plastic zone), and is based on stress concentrations and the crack length. Therefore this stress amplitude is constantly increasing during the simulation process, as the crack propagates.

For zone 4 it is postulated that a simple superposition of the crack propagation rates in eq. [2] and eq. [3] can be used, as both fatigue regimes are active in this zone. Therefore:

$$(da/dn)_4 = (da/dn)_2 + (da/dn)_3 \tag{4}$$

Instead of simple addition, weight functions could be used, but in our study the plain addition was preferred and good fit by the simulations were achieved for metal parts. It was not considered nor tested for other materials.

The material parameters C_2 and C_3 were calibrated by curve fitting to experimental results, but then were kept constant, and gave good predictions for subsequent tests and simulations.

Zones 5 and 6 are in the plastic range, and a basic study about the crack propagation here has to be further enlarged. It is not a central issue for the engineering field, as structures are mostly designed not to operate in these zones, but it is an important academic and scientific field. In our study we used equation [4] also as first approximation for zone 6. It most probably did not alter much, as the number of crack propagating cycles here was small compared to the whole fatigue life.

Calculation and demonstration of various fatigue phenomena

The calculation model presented here, and the Fatigue Diagram have been used to analyze, explain and demonstrate a few known fatigue phenomena, like the High-Low and Low-High loading sequence effect, crack arrest, overstressing, influence of mean stresses, influence of surface finish, calculation of S-N curves etc. These studies have shown that the proposed model can be used to quantitatively predict and explain all of these phenomena. Due to lack of space only two of these effects will be reviewed here, the general exhibit of crack propagation and the sequence effect. The demonstration of the crack size in each propagating stage and cycle is displayed in figure 2.

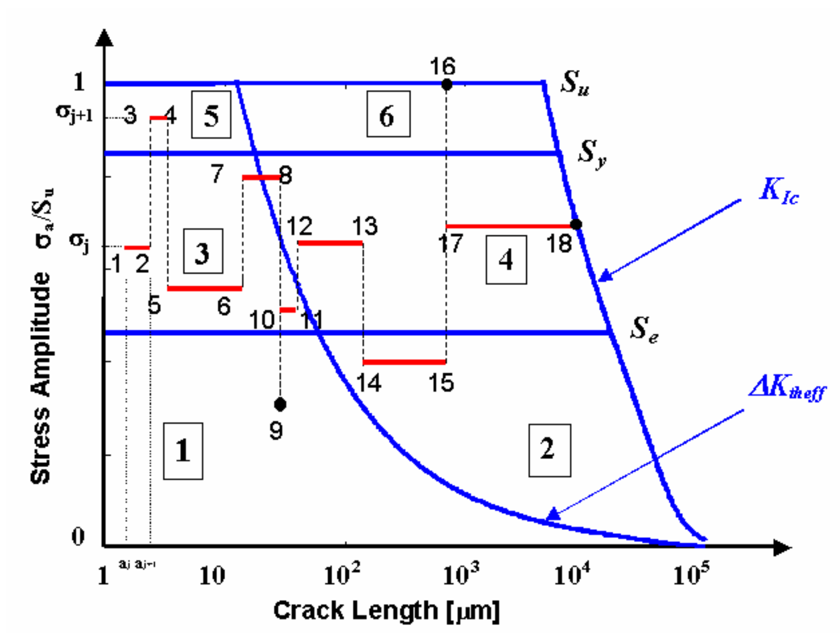

Figure 2. The general fatigue diagram for a round tension-compression specimen with a side crack, that propagates by a nine steps programmed block loading, from 2 microns (point 1) till about 16 mm (point 18) at fracture. [7]

One can see that the initial micro-crack a_j is of the size of about 2 microns (point 1). The specimen is loaded with a block of loading cycles with stress amplitude σ_j and no mean stress, i.e. R=-1. The crack propagates in zone 3 from point 1 to point 2 to the length a_{j+1}. The CPR can be calculated by equation [3]. Now the stress amplitude is elevated to σ_{j+1} and another block of cycles is actuated. The crack propagates from point 3 to point 4 in the low cycle plastic regime. The propagation was calculated, as a first approximation, by using equation [3]. Now the stress amplitude is lowered to point 5 and the propagation proceeds till point 6. When the crack propagates from point 7 to 8, the process crosses the threshold line and therefore the calculation has to start with equation [3] and switch to equation [4] at the transition point. The next block is in stress amplitude lower than the endurance limit, as seen in point 9. The crack arrests and does not propagate. Then again, the propagation proceeds in blocks 10-11 and 12-13. The following block 14-15 is in the LEFM regime and equation [2] is used. The stress amplitude can now be elevated to point 16 where fracture after gross yielding occurs, or alternatively to point 17 and the specimen will fracture by critical crack propagation at point 18. The whole procedure has been simulated on a computer, to calculate the correct CPR in each loading block. A singular diagram must be drawn for each specimen and loading geometry.

In Figure [2] one can see clearly several important fatigue phenomena. The crack propagation switches from one regime to another in loading line 6-7 and then back at line 10-11, it arrests the crack in loading point 9, it gets back into LEFM zone 2 in loading line 14-15 and finally suffers critical propagation at point 18, or eventually gross yielding at point 16, if the stress amplitude was lifted to this level. The crack propagation can be calculated and displayed on the diagram for mean stresses as well, as detailed by Peles and Weiss [7].

The sequence loading effect has been known for a long time. It was not quantitatively used for crack propagation, but rather experimental results were displayed on graphs with number of High and Low cycles used as the axes. The effect has been analyzed by Weiss and Hirschberg [4] using the proposed model and typical results are depicted in Figure [3].

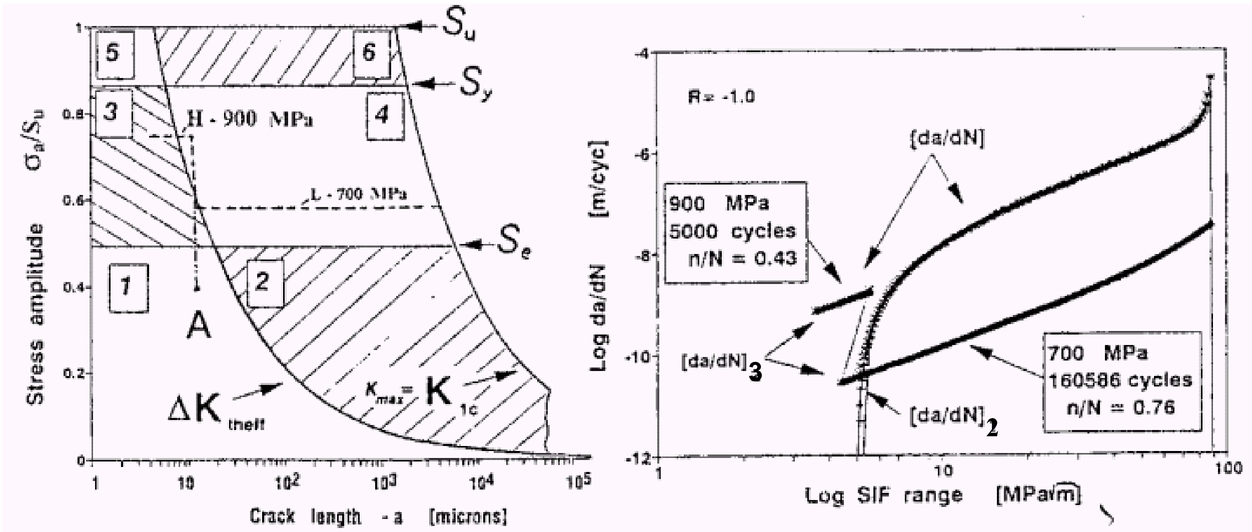

Figure 3. A High-Low sequence loading depicted on the fatigue diagram and on a da/dn curve. 5000 cycles of 900 MPa were used as the High load and then 160586 cycles at 700 MPa were needed to fail the specimen. Total n/N was 0.76 [4].

In Figure [3] the High-Low cycling effect is depicted. The total relative number of cycles needed to fail the specimen, in two levels of stress amplitude, was 0.76. A reversed cycling of stresses was simulated with a Low-High sequence. First 266,000 cycles at 700 MPA were applied, with n/N = 0.53, and then the test was continued at 900 MPa, and 7813 cycles were needed till failure. The total n/N was 1.25. Many other combinations of different levels of L-H sequences have been simulated, and the final summation was consistently higher than 1. One can see in the right part of Figure [3] the crack propagation rates in zone 3 depicted as $(da/dN)_3$ and the others in zone 4 which are a linear combination of $(da/dN)_3$ and $(da/dN)_2$, and shown as the upper lines (da/dN). In experimental results depiction it is easy to miss the distinction between the two types. The important result is that in H-L prediction the total n/N sum is always less than 1 and in the L-H sequence it is always higher than 1. These results are valid when the stress amplitudes are below S_y. The possible stress arrest effect is depicted in point A in the left side of Figure [3]. Other fatigue phenomena can be explained using Figures [2] and [3].

The model applied to fatigue assessment of steel wire ropes

The wire rope serves as a load carrier device in hoisting appliances, elevators and as a structure element in suspended bridges, cranes and offshore plants. The rope is constructed of laid wires and strands that provide the rope's flexibility and strength. Wire ropes are extremely complicated machine elements, and their main failure mode is fatigue. In most cases a few outer wires will tear and when a certain number of torn wires have been accumulated in a specified cable length, the rope has to be discarded. The wires are built as double helix structures and the exact stress analysis of the double helix geometry has been solved by the authors only recently, Elata et. al. [8]. In the past only experimental fatigue results in wires were available. Now, with availability of the exact stress functions and the two-term fatigue model, simulations and good predictions of the fatigue life of single wires, have been performed by Ashkenazy [9]. The preformed double helix wire contains significant residual stresses that were generated during the manufacturing process in tension and in twisting, even before any load has been applied. Then the wire is loaded in tension under load, in bending when passing over a sheave, in shear stresses due to twisting, in friction and pressure between adjacent wires and the sheave surfaces and in secondary local bending. The current fatigue model deals with a combination of tension and bending only, in both parts of the calculation procedure, according to equation [4]. Shear stresses and fretting fatigue due to friction and wear in the wire have not been considered.

The stress analysis in a double helix wire is extremely complicated and will not be described here, it was fully detailed in the references [8;9]. As a very frequent fatigue problem in industry, a small number of results of the fatigue simulations, based on the stress analysis, will be shown and compared to a few of the many available experimental results. A typical hoisting apparatus that is part of many crane structures is depicted in Figure [4]. On the right side the structure of the hoisting device is shown, including the 4 reeve system on which the load W is suspended. As the wire rope passes around the sheaves, a few additional bending stress cycles are added to the existing tension stress. On the left, the varying stress in one certain point of the wire, which passes around the sheaves is depicted, for one full hoisting and lowering cycle. The stresses are not shown to exact scale, actually the additional bending stress in the wire of a crane appliance, due to the bending on the sheave, is about twice as high as the value of the tension stress due to load W, and therefore is the main factor in the loading cycle, the mean stress and life estimation. One can see that in each hoisting cycle depicted in figure [4], about 8 bending cycles of the wire are generated. They were counted using the rain-flow method of fatigue cycles analysis. The counted loading cycles were used for

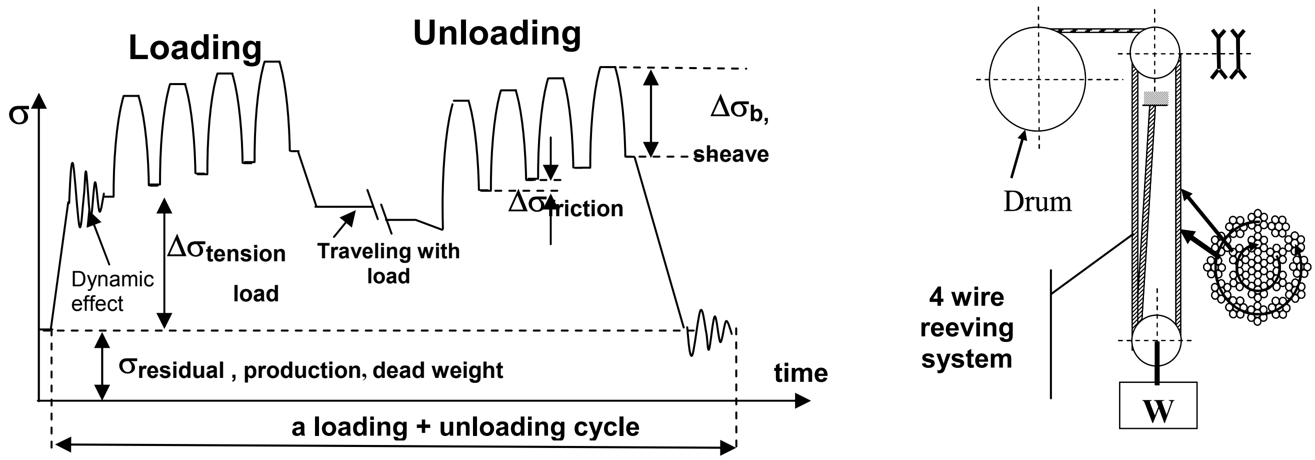

Figure 4. A typical hoisting system where the load is suspended on 4 wires is depicted on the right side. The tension and bending stress values σ_i in one loading and unloading cycle, as the wire passes around the sheaves, is shown on the left.

the evaluation of crack propagation in a single wire with an initial crack – a_0 that was generated during the production deep drawing of the wires. The equivalent initial cracks were considered to be penny-shaped, and the calculation of the crack propagation was performed accordingly. The initial depth of the indentations in the single wires were found by Lorka [10] to be in the order of magnitude of 20 to 50 microns, so that the whole fatigue life is taking place in zone 4. The average breaking (bending) fatigue stress, as reported by Feyrer [11], is close to the simulated values, as calculated by Ashkenazy [9].

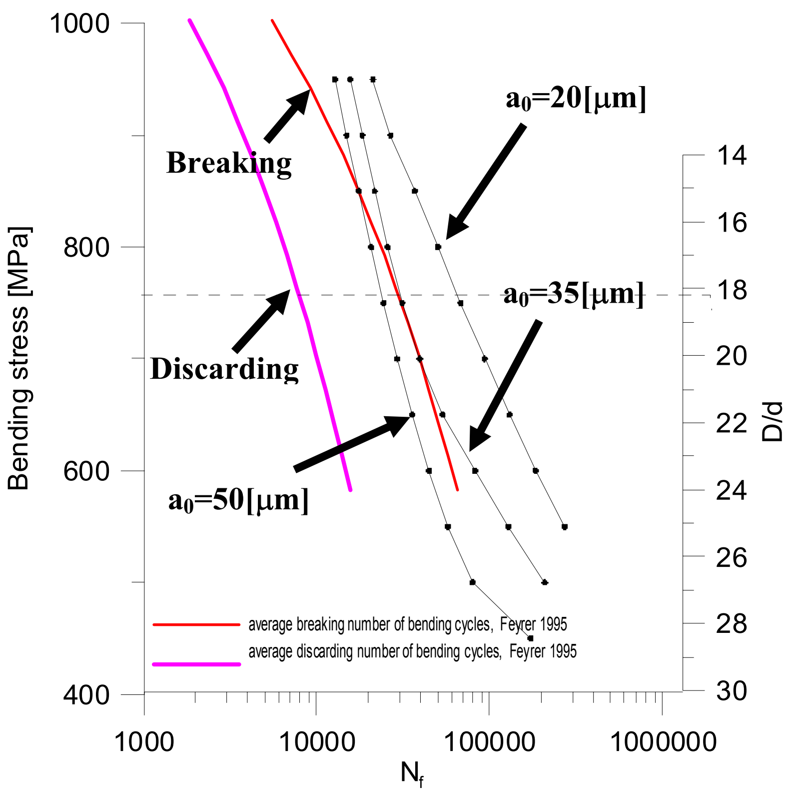

Figure 5. The simulated S-N curves for different initial crack length a_0 and the experimental results by Feyrer, exhibiting the average number of bending cycles till the final failure of the wire, and the safe discarding criteria.

Conclusions and discussion

1. The whole fatigue domain has been depicted on one comprehensive diagram, and used to define 6 fatigue zones and regimes. The regimes have been defined, based on the combination of crack length and stress amplitude only, and every point in them is calculable and measurable. The popular term "fatigue damage" has not been used, as it is not experimentally measurable.
2. A calculation model that includes the two modified relations for crack propagation estimation, has been proposed and used separately for zones 2 and 3 in the fatigue diagram. One material parameter has to be calibrated by experiments in each relation, but once so adjusted, the use of the relations yields very close predictions to experimental results, in various specimen types and loading conditions.
3. It is postulated that, as part of the calculation model for crack propagation predictions in zone 4, a superposition of the two relations used in zones 2 and 3 has to be used. In this zone, predictions by many proposed calculation methods tend to substantially deviate from measured results. The use of the proposed combination of crack propagation relations yields good fit with experimental results.
4. The model has been used to calculate and predict S-N curves, to calculate and understand the fatigue behavior of smooth metal specimens, to explain the H-L and L-H sequence effect, to explain crack arrest and additional known fatigue phenomena. The validity of use of the model has been shown in the past for smooth tension-compression and for bending specimens, explicitly for mode I elements. It has to be considered and tested in other stress combinations.
5. In the current study the model has been shown to fit to complex steel wire ropes, and enabled for the first time to predict the fatigue life of single wires in practical use, and evaluate safe life of wire ropes and their discard criteria.

Acknowledgment

This research was partly sponsored by the Fund for Preemptive Action of the Israeli Ministry of Commerce, Industry and Labor.

References

1. Miller K. J. "Materials Science Perspective of Metal Fatigue Resistance" , Materials Science and Technology **9**, 453-462, (1991).
2. Miller K.J. "Initiation and Propagation of Short Fatigue Cracks", Proc. of Fatigue'96, Berlin, 253-264, Pergamon (1996)
3. Taylor D. and Clancy O.M. "The Fatigue Performance of Machined Surfaces", Fatigue and Fracture of Engineering Materials and .Structures **14** (2/3) 329-336 (1991).
4. Weiss M.P. "Estimating Fatigue Cracks, from the Onset of Loading, in Smooth AISI 4340 Specimens, under Cyclic Stresses", Int. J. Fatigue **14** (2), 91-96. (1992)
5. Weiss M.P. and Hirshberg Z. "Crack Extension under Variable Loading in the Short and Long Crack Regime, using a General Fatigue Diagram", Fatigue and Fracture of Engineering Materials and .Structures **19** (2/3) 241-249, 1996
6. Kitagawa, H. & Takahashi, S. Proc. 2nd Int. Conf. on Mechanical Behavior of Materials, Boston, ASM, 627-631, (1976)
7. Peles S. and Weiss M.P., “A modified Two-Term Fatigue Life Prediction Model for Mean Stresses in Steel”, in FATIGUE’99, Proceedings of the seventh International Fatigue Congress, Beijing, June 1999, pp. 857-864.
8. Elata D., Ashkenazy R. and Weiss M.P. "The Mechanical Behaviour of a Wire Rope with an Independent Wire Rope Core", International Journal of Solids and Structures, 2004, Vol 41/5-6 pp 1157-1172
9. Ashkenazy R. "Fatigue of Steel Wires", PhD Thesis, TECHNION IIT, (2004)
10. Llorka J. and Sanchez-Galvez V. "Fatigue Threshold determination in High Strength Cold Drawn Eutectoid Steel Wires", Engineering Fracture Mechanics, **26**, No. 6 869-882, (1987)
11. Feyrer K. Drahtseile, Springer-Verlag, Berlin (1994)